Efficient Space-Time Finite Elements for Thermo-Mechanical Problems

K.Quaine[1,2], H.Gimperlein[1], J. Stocek[1,2], Andrew Lacey[1]

[1] Department of Mathematics, Heriot-Watt University, UK.
[2] School of Mathematics, University of Edinburgh, UK.
kq8@hw.ac.uk, h.gimperlein@hw.ac.uk

Abstract

This talk discusses efficient and reliable Finite Element Methods to simulate the thermo-mechanical response of high explosives. A key motivation is the modelling of the initiation of shear bands in materials such as HMX. The localised plastic deformation associated with a shear band leads to the formation of hot spots and can subsequently lead to thermal runaway. Standard finite element methods struggle to accurately resolve the sharp variations associated with these thermal and mechanical features which may lead to unphysical predictions of the numerical models. The numerical methods presented in this talk aim to provide efficient and reliable tools towards modelling the initiation of shear banding and thermal runaway. We consider two approaches: adaptively generated meshes based on mathematically rigorous estimates of the numerical errors, and enriched finite elements. They are illustrated for thermal and elastic problems, as they arise in reduced models. We first, we present results based on adaptive finite elements for non-linear thermal problems. Steep temperature gradients are resolved by appropriate mesh refinement procedures. Steered by indicators for the accuracy of the solution, the algorithm automatically resolves hot spots on a refined mesh, significantly reducing computational costs, see for example [6]. Secondly, we consider enriched space-time finite elements (also known as generalised finite elements) which include a priori physical information into the numerical method. This a priori information could represent localised of wave-like features, which are added to a coarse approximation space. The modelling can effectively capture features occurring at different spatial and temporal scales [10, 14]. Here we consider a first order formulation of the wave equation [1] and choose plane-wave enrichments [16]. Future work aims to address the full, coupled thermo-mechanical system, as well as to combine the adaptive and enriched approaches of Iqbal et al. [9].

Key words: *Generalized Finite Elements; Adaptive Finite Elements; Space-Time Methods; Plane-Wave Enrichment.*

1 Introduction and Motivation

Improper handling of energetic materials, such as accidental mechanical or thermal insults, may lead to thermal runaway with its potentially disastrous consequences, as seen in Beirut disaster on 4th August 2020 [5, 17]. Of particular interest is the initiation of shear bands, a strain-localisation phenomenon which is expected to play a role in HMX plasticity. The localised plastic deformation leads to the formation of hot spots, which may subsequently cause ignition on time scales long after an initial mechanical insult. While experiments can provide insights into the dynamical evolution, they are limited by experimental, financial and safety constraints. Mathematical models may provide qualitative and quantitative means to determine the behaviour of a material under an insult, taking into account the coupled mechanical, chemical and thermal dynamics inside the energetic material. They may predict the internal deformation and the location and time scales of a potential ignition [7]. To understand and quantitatively predict key mechanisms of the onset of a reaction in an energetic material, based on a mathematical model, requires efficient and reliable numerical methods. Current hydrocodes can fail to represent the extreme localised thermal and mechanical effects in shear bands, due to the severe temperature and strain gradients associated with these problems [15]. For example, [15] discusses the failing of various numerical packages when modelling shear bands. It is further of interest to separate the uncertainties of the mathematical from the challenges of its numerical simulation. We here present preliminary results for

two complementary numerical approaches based on advanced finite element methods. *Adaptive finite elements* efficiently resolve localised features by automatic mesh refinements in the regions of large numerical error. The underlying a posteriori error estimates allow us to quantify the accuracy of the numerical result and refine it until a prescribed tolerance is achieved. This is illustrated in recent work [6] on contact problems corresponding to a mechanical insult or friction. We here describe its analogue for situations potentially leading to thermal runaway. The second numerical approach, *enriched finite elements* (EFEM), allows us to include available physical information into the numerical approximation spaces. Such information about the solution may circumvent the numerical difficulties and in this way achieve engineering accuracy with a numerical cost reduced by orders of magnitude [8, 4]. The approach we present here relates to recent work on Trefftz methods [1, 13].

To be specific, we consider thermo-mechanical models relevant for energetic materials of the form of a heat equation

$$\rho C_v \frac{\partial u}{\partial t} = \sigma_{ij}\dot{\varepsilon}_{ij} + \rho\dot{r} + \kappa\Delta u \tag{1}$$

for the temperature u. Here $\dot{r}$ is the rate of heat, per unit mass, being produced by a chemical reaction in a material, κ the thermal conductivity, ρ the density and C_v the specific heat capacity. The mechanical properties $\dot{\varepsilon}$ and σ_{ij} correspond to the strain rate, respectively the stress. As governing equations for the mechanics, a combination of non-linear elastic and viscous behaviour may be relevant. Bebernes and Lacey [2] discuss such models for shear banding and Ohmic heating. By integrating the mechanical problem analytically for specific geometries, [2] derives effective non-linear heat equations of the form

$$\frac{\partial u}{\partial t} - \Delta u = \lambda r(u) + g(u) \cdot \left(\int_\Omega g(u)\mathrm{d}\Omega \right)^{-p}, \tag{2}$$

where the non-local, non-linear term g is determined by the temperature dependence of the mechanical properties. In this way, a large class of heat-like equations is obtained, and their efficient numerical approximation becomes relevant. On the other hand, we consider elastic problems under a localised point insult. To illustrate our approach, the model problem of the scalar wave equation is considered. Extensions to elastic problems will be addressed in future work.

2 FEM Set Up and Discontinuous Galerkin Formulation

In the following sections we will be discussing the two methods mentioned above: Adaptive FEM and EFEM. To do this effectively we will be considering the basic set up of both methods initially and then discussing how we extend from a standard FEM method into these more complex regimes. We will be considering toy mathematical problems in the form of a heat equation for adaptive FEM and an acoustic system in EFEM.

2.1 Thermal Problem

First we discuss the set up of a standard and then adaptive FEM scheme. The theory of finite element method approximations again follows that which is detailed in [18] and its implementation as a MATLAB algorithm was largely informed by [11]. For a convenient example let us consider a heat equation,

$$\frac{\partial u}{\partial t} - \Delta u = f(u), \tag{3}$$

where the temperature u maybe be dependent on space and time. Now we give a general template for FEM. To do this we follow a five step approach to obtain an approximate solution to the variational form:

1. Reformulate the PDE into variational form

2. Discretise the domain, $Q = \Omega \times [0, T] = \Omega \times \mathcal{T}$, into elements

3. Define a suitable basis for S_h given the discretisation

4. Generate the system of algebraic equations

5. Solve the system and obtain the approximate solution.

In step one we are tasked with finding the variational formulation

$$\int_\Omega u_t v + \int_\Omega \nabla u \cdot \nabla v = \int_\Omega f(u)v \tag{4}$$

where v is a *test function* such that $v \in H_0^1$.

Step 2 of the process, discretising $\overline{\Omega}$, is done by splitting the domain into a finite family of disjoint elements. This discretised domain shall be denoted by $\mathcal{T}_h$ and the nodes by N_h. The collection of these nodes are denoted as $\{P_i\}_{i=1}^{N_h}$. We know that the variational solution, u, belongs to H_0^1 and that this is an infinite dimensional space. The aim to approximate u from an N_h-dimensional subspace S_h. To the ith node, P_i, we assign a piecewise linear function, ϕ_i which takes the value 1 at P_i and 0 otherwise. The set $\{\phi_i\}_{i=1}^{N_h}$ defines a basis (in our case piecewise linear) for the subspace S_h, from which we shall approximate the solution of (4). This approximation shall be defined as $u_h \in S_h$ and clearly for some $\{\alpha_i\}_{i=1}^{N_h}$, such that $\alpha_i : (0, T] \to \mathbb{R}$ for all $i \in \{1, ..., N_h\}$, we have

$$u_h(., t) = \sum_{i=1}^{N_h} \alpha_i(t)\phi_i, \tag{5}$$

for some fixed t. Now we substitute this approximation into equation (4). Note, every basis function ϕ_j belongs to H_0^1 and as a result constitutes a suitable test function.

For the discrete parabolic problem we introduce the space-time bilinear form $B_{DG}(\cdot, \cdot)$ given by

$$B_{DG}(u, v) = \sum_{k=1}^{N_h} \int_\mathcal{T} \langle \partial_t u, v \rangle + \Delta(u, v) \mathrm{d}t, \tag{6}$$

whereby we immediately draw the weak formulation,

$$B_{DG}(u_{h\tau}, v_{h\tau}) + \sum_i^{N_h} \langle u_{h\tau}^-, [v_{h\tau}] \rangle_\Omega = \langle f, v_{h\tau} \rangle_Q, \tag{7}$$

for τ the particular time step in $\mathcal{T}$ and where $[\cdot] = [v_h n_t^+ + v_h n_t^-]$ represents a jump in time for $+$ being from above and $-$ from below. Now, since (7) holds for each $j \in \{1, ..., N_h\}$, for every fixed $t > 0$ we have a system of equations. This can be written more compactly as the matrix equation

$$\mathbb{I}(\alpha(t + h) - \alpha(t)) + A\alpha(t + h) = \mathbf{F}(t). \tag{8}$$

The matrices $\mathbb{I}$ and A are each $N_h \times N_h$ matrices. As mentioned previously the matrices $\mathbb{I}$ and A are called the *mass* and *stiffness* matrices respectively and the vector $\mathbf{F}(t)$ is referred to as the *load vector* [18].

2.2 Wave Propagation of an Elastic Problem

As discussed in Section 1 we will also be considering enriched finite elements for an acoustic system. The motivation behind focusing on the acoustic wave equation is because of its practical applications - ranging from deformation in energetic materials to railways and tidal power. In this paper we will be considering the first order acoustic system,

$$\begin{cases} \dfrac{1}{c^2 \rho} \dfrac{\partial p}{\partial t} + \nabla \underline{v} = f_1 \\ \rho \dfrac{\partial \underline{v}}{\partial t} + \nabla p = f_2 \\ p(\cdot, 0) = v(\cdot, 0) = 0 \\ p_t(\cdot, 0) = v_t(\cdot, 0) = 0 \end{cases}, \tag{9}$$

where we have unknowns as the pressure (p) and velocity ($\underline{v}$) with constants of density (ρ) and acoustic wave speed (c). For this preliminary work we will consider these constants as 1, to ease the numerical experimentation. Before continuing on we should point out the acoustic equation above can easily be re-written as the wave equation by differentiating with respect to space in one PDE and time in the other. Once we do this we can eliminate the common term to form the wave equation,

$$\frac{\partial^2 p}{\partial t^2} - \Delta p = f. \tag{10}$$

Our work first starts to differ in the initial stage of the the set-up when compared to a standard FEM scheme. We pose the above system in the following space-time domain, $Q = \Omega \times [0, T]$ - where Ω is the spatial domain and T is the final time. We further require that each element, $\mathbf{K}$, must be a subset of Q and thus spans both spatial and temporal nodes. The main advantage of this is to allow us to enrich in both space and time, unlike the previous works discussed in Section 1.

Now that the preliminaries have been set up, we should consider how we formulate the problem. From (9) we find that the weak formulation is, noting that $\underline{\eta}$ and q are the test functions,

$$\sum_{\mathbf{K}} - \int_{\mathbf{K}} p \frac{\partial \overline{q}}{\partial t} + \underline{v} \cdot \nabla \overline{q} \, \mathrm{dV} + \int_{\partial \mathbf{K}} p^- [\overline{q} n_t^+ + \overline{q} n_t^-] \mathrm{ds} = \sum_{\mathbf{K}} \int_{\mathbf{K}} f_1 \overline{q} \, \mathrm{dV}, \tag{11a}$$

$$\sum_{\mathbf{K}} - \int_{\mathbf{K}} v \frac{\partial \overline{\underline{\eta}}}{\partial t} + p \nabla \cdot \overline{\underline{\eta}} \, \mathrm{dV} + \int_{\partial \mathbf{K}} v^- [\overline{\underline{\eta}} n_t^+ + \overline{\underline{\eta}} n_t^-] \mathrm{ds} = \sum_{\mathbf{K}} \int_{\mathbf{K}} f_2 \overline{\underline{\eta}} \, \mathrm{dV}, \tag{11b}$$

where $\underline{\eta}$ is now a vector of two variables (η_1, η_2). This subtle change to the weak formulation requires extra care when we compute these relevant gradients and divergences. Now we should note that we will be considering the enriched finite element method in 2.5 dimensions. Now we define the ansatz function for the pressure (noting the approximation for the velocity and the test functions are analogous),

$$p_h(\underline{x}, t) = \sum_m^{\tilde{T}} \sum_b^Q P_m \Pi(t)_m G_{j,m}^{(b)}(x, t). \tag{12}$$

This is easily derived from the general FEM formulation (Section 2.1), with the multiplication of an enrichment function $G(x, t)$,

$$p_h(\underline{x}, t) = \sum_m^{\tilde{T}} \sum_{i,j}^N \sum_b^Q P_{j,m} \Lambda_{i,j}(\underline{x}) \Pi(t)_m G_{j,m}^{(b)}(x, t), \tag{13}$$

where we include summations for space to account for the piecewise linear hat functions, $\Lambda_{i,j}(\underline{x})$. To arrive at (12) we simply need to bring the summation through onto the spatial hat functions, noting that $\sum_{i,j} \Lambda_{i,j} = 1$. We can easily apply the same idea to the matrices of the system. A reasonable question, at this point, is why would we want to remove the spatial hat functions? This

is because we are computing a two-dimensional Fourier series, where P_m is a Fourier coefficient. As a result we are able to use a Fourier series approximation to populate a solution for all nodes in the problem. By this we mean that we take one node in space, due to the removal of the hat functions, and then solve the system with the appropriate enrichments before generalising the Fourier modes into solutions for any given domain.

3 Adaptive FEM

There are many reasons as to why adaptive FEM this is beneficial over standard finite elements. For example if we consider the heat equation,

$$u_t - \Delta u = \delta u^2, \tag{14}$$

where we are able to choose conditions such that we are guaranteed blow-up.

If we expect there to be some sort of event occurring, such as blow-up, within the material then we might find that a standard finite element method will not be able to resolve an accurate solution at these points of interest. As a result we would expect to see large errors caused by the steep gradients (or jumps) between elements. This is where adaptive mesh refinements comes into its own. It is able to deal with these challenging gradients and will cluster mesh refinements around these points and accurately approximate solutions.

3.1 A Posteriori Error Estimates

To be able to implement adaptive mesh refinements we must first have an understanding of the errors associated with each element in the mesh. For this section we will neglect all the theory behind computing the error indicators but would like to direct you to Iqbal et al. [8] who discusses a-posteriori errors for the h-method. In this vein we will simply state the a-posteriori error used in the numerical experiments.

Theorem 1 (A Posteriori Error Indicators [6])**.** *Let $u, u_{h\tau}$ be solutions of parabolic problem. Then we define $\sigma_{h\tau}$ and residual r_{h_τ} to be the discrete counterparts of σ and r given by in the space $H_0^1(K)$ such that,*

$$\langle \sigma_{h\tau}, v_{h\tau} \rangle = \langle f, v_{h\tau} \rangle - a(u_{h\tau}, v_{h\tau}) - \langle \partial_t u_{h\tau}, v_{h\tau} \rangle, \ \forall v_{h\tau} \in \mathbb{W}_{h\tau}(0, T) \tag{15}$$

$$r_{h\tau} = f - (-\Delta)^s u_{h\tau} - \partial_t u_{h\tau}. \tag{16}$$

Now assume that $f \in H_0^1(K)$ and $\chi \in \mathbb{V}_h \subset H_0^1(K)$. Then the following computable abstract error estimate holds

$$||(u - u_{h\tau})(T)||_{L^2(\Omega)}^2 + \int_0^T ||u - u_{h\tau}||_{H_0^1(\Omega)}^2 + ||\partial_t(u - u_{h\tau})||_{H^{-s}(\Omega)}^2 + ||\sigma - \sigma_{h\tau}||_{H^{-s}(\Omega)}^2 \, dt$$

$$\lesssim ||(u - u_{h\tau})(0)||_{L^2(\Omega)}^2 + \int_0^T ||\tilde{u}_{h\tau} - u_{h\tau}||_{H_0^1(\Omega)}^2 + ||r_{h\tau} - \sigma_{h\tau}||_{H^{-s}(\Omega)}^2 \, dt \tag{17}$$

3.2 Implementation

In this subsection we will discuss how we have implemented the errors and mesh refinements into MATLAB. We start by considering the refinement procedure: Solve; Estimate; Mark; Refine. However, we will be giving a brief explanation on how the code works. We start by giving a brief outline of the Adaptive Finite Element algorithm:

Adaptive Algorithm

1. Set up the problem

   - Create a coarse mesh
   - Define the accuracy level that is desired

2. Solve the linear system

3. Compute the error indicators for each element

   - Stop iterating if the desired accuracy is attained

4. Mark the elements in need of refinement

5. Refine the marked elements

6. Repeat the process from (2)

Applying the above algorithm to an arbitrary example we can demonstrate how the refinement happens on a mesh. The process will either use red, green or blue refinement (Figure 1a) in each iteration prior to the error being smaller than the desired error (Step 4). First we will see red refinement and the two adjoining green edges - accounting for the hanging nodes. In the second iteration we see that the green refinements are removed to allow for the error to be recomputed with shape regular triangles. This leads to red-green-blue refinement and then in the final iteration we see red-green-red refinement. During the refinement stages we should expect to see that the

(a) Initial mesh. (b) Red refinement. (c) Green refinement. (d) Red-Blue refinement. (e) Blue-Red refinement.
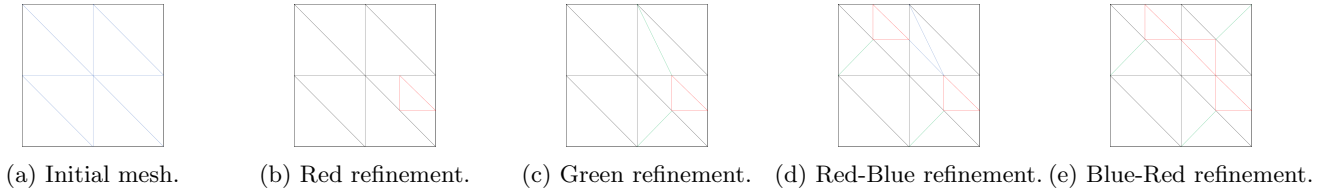
Figure 1: Example of a refinement procedure.

error associated with the solution decreases after each iteration. We should also note that in (c) we connect the hanging (free) nodes to the nodes from the original mesh. The reason for this is due to the definition of FEM and this will help enforce shape regularity with later iterations.

4 Enriched Finite Elements

To fully understand and use an enriched method appropriately one of the key criterion is to know some qualitative behaviour behind the problem we wish to solve. For example, we might choose to enrich the system with Gaussian functions if we have a heat problem - as seen Iqbal et al. [8]'s experimentation. For the problem that we are considering, we can naively choose the enrichment functions to be plane waves [16], recalling that we are considering the acoustic system (9). The reason for this is quite simple, if we expect the solution to travel in the form of a plane wave, it is logical to seed the initial finite element scheme with functions that can accurately approximate physical nature of the problem (for other examples see Iqbal et al. [8] paper on *An a posteriori error estimate for the generalized finite element method for transient heat diffusion problems*). As a result we take,

$$G^{(\underline{b})}(\underline{x}, t) = \exp(i(\underline{k}^{(b)}\underline{x} + \omega^{(b)}(t - t_0))) = \exp(i(k_1^{(b_1)}x + k_2^{(b_1)}y + \omega^{(b)}(t - t_0))), \qquad (18)$$
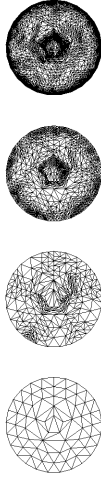
where $\underline{k} = (k_1, k_2)$ are the wavenumbers, ω is the frequency and $\underline{b} = (b_1, b_2) \in \mathbb{Z}$ represents the differing combinations of enrichments. We should further establish that one must make a

symmetric choice in the wavenumbers and the frequency. This means that for every $k, \omega > 0$ we also chose its corresponding negative value such that $-k, -\omega < 0$. The reasoning behind this is it allows one to choose a larger number of frequencies as well as removing the complications from the additionally complex terms that are present within the enrichments. As a result the we have eight different combinations for k_1, k_2 and ω. We should note that we choose the wavenumbers in a regular grid pattern such that the difference between each entry is $\dfrac{2\pi}{L}$ where L is the length of the edge in a square domain - this can be generalised into more complex domains.

5 Numerical Experiments

5.1 Adaptive FEM

Here we will consider the applications of adaptive finite elements to a heat equation in a qualitative manner. We will see that the problem being considered has the introduction of a thermal insult in the centre of the circular domain, we should expect that the heat diffuses across the domain, in a somewhat uniform radial manner. If we first consider the static problem in a circular domain and with an initial condition of 0. Here we see how the static problem reacts to the introduction

(b) Convergence of the error for different methods.

(a) Mesh refinements in space at time t.

of a thermal insult. In the image we can that there is some clustering around the centre of the mesh, where the insult occurs. This is evidenced over four iterations above as we see the density of the mesh increasing in each step. We then see from Figure 2b that there is clear convergence within this method and that it is significantly quicker than the uniform FEM case. We see that the rates of convergence for the adaptive FEM is $\frac{3}{8}$ compared to the uniform case of $\frac{1}{4}$ so there is a significant speed increase on this method as expected. We can clearly see that there is a substantial increase over time, when $\dfrac{\partial u}{\partial t} \neq 0$.

Now if we consider the problem over time we see that the mesh refines in space (in the horizontally) and in time (vertically).

We clearly see, as expected, that the meshes will refine rapidly in time when the insult occurs; we expect a rapid increase in the number of elements around the *impact* point. This is expected as one would reasonably think that the error will increase at this time. Then when the heat transfer
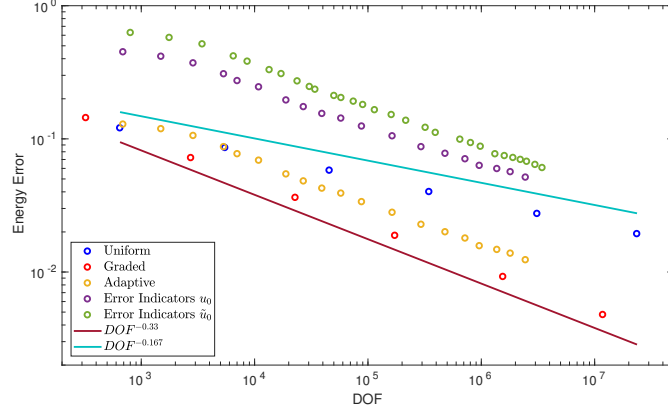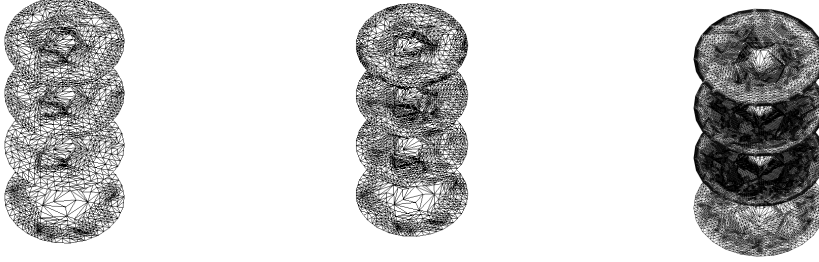
Figure 3: Error in the energy norm.

Figure 4: Adaptively refined meshes after $3, 8, 15$ refinements at $t = 0, 0.4, 0.8, 1$, from bottom to top, respectively.

disperses we start to see some coarsening in the meshes as we no longer have the large errors which are found in the steep temperature gradients between elements. We can see that this refinement occurs in the following error plot.
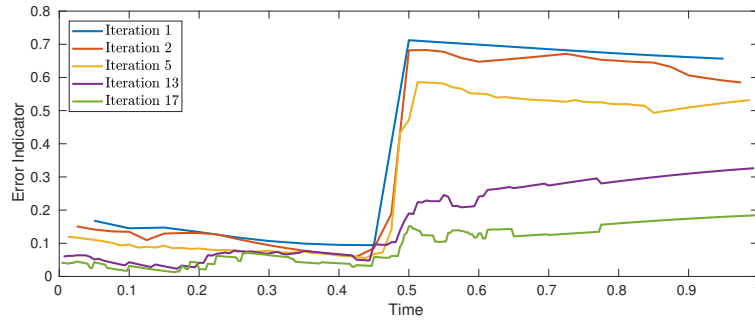

Figure 5: Error indicators of adaptively refined meshes in time with the initial condition given by $\tilde{u}_0$.

5.2 Enriched FEM for Wave Propagation

5.2.1 Gaussian Impact

Now we consider an applicable application in the form of a Gaussian Impact. We first define system (9) with the right hand side,

$$f(x, y, t) = \begin{cases} f_1(t) f_2(x, y) \begin{cases} 0 < t < 2t_0 \\ (x - x_0)^2 + (y - y_0)^2 < R^2 \end{cases} \\ 0 \end{cases}, \tag{19}$$

where f_1 and f_2 give by [3],

$$f_1(t) = 4 \exp\left(-\pi^2 f_0^2 (t - t_0)^2\right), \tag{20a}$$

$$f_2(x, y) = \left(1 - \frac{(x - x_0)^2 + (y - y_0)^2}{R^2}\right)^3. \tag{20b}$$

Here $t_0 = \frac{1}{f_0}$, $f_0 = \frac{c_0}{h N_L}$ is the central frequency, N_L the number of points per wavelength, h is the mesh size and c_0 is the wave-speed. Qualitatively this function represents a circular source centred at (x_0, y_0) which emits radial waves until the time reaches $t = 2t_0$ and these will travel throughout the domain before *reflecting* (noting that the boundary conditions are periodic) back into the emitting wave - this will show the complex structure of interference patterns. This type of problem could therefore be related to many aspects in the real world, for example these could be in a mechanical regime whereby we might have an explosion or impact which expels a pressure wave. In this section we hope to show convincing evidence that a Fourier scheme could be effectively used to tackle these sorts of problems. We will look to compare the solutions from both a space-time enrichment as a space enrichment. To do this we by setting the scene of the numerical experiment for a square domain $\Omega = [0, 2\pi]^2$. The pressure wave we expect to see from this should be radial and should travel outwards from a central impact point - we take $x_0 = \pi$, $y_0 = \pi$ and $R^2 = 0.25$. This means that the source term could be imagined to model a mechanical insult on the material, as seen in a Steven or Spigot test (Figure 6). Now these tests, taken from Collino and Tsogka [3]
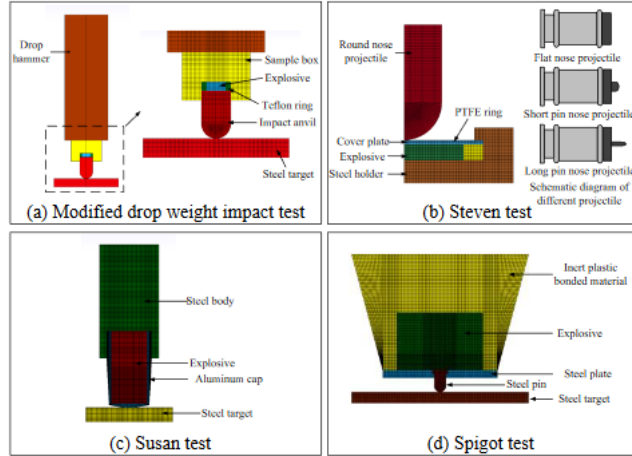

Figure 6: Low velocity impact tests on explosives [12].

show the global interaction between an impact and the corresponding material used. We believe that a function, such as the Gaussian Impact might be suitable to model such a problem on a local level. Now with the application in mind we consider how enriched finite elements will model this with both space and space-time enrichments. Now if we initially consider some preliminary

spatial enriched plot we see the following progression over time but we consider the insult when it occurs over a long period of time.
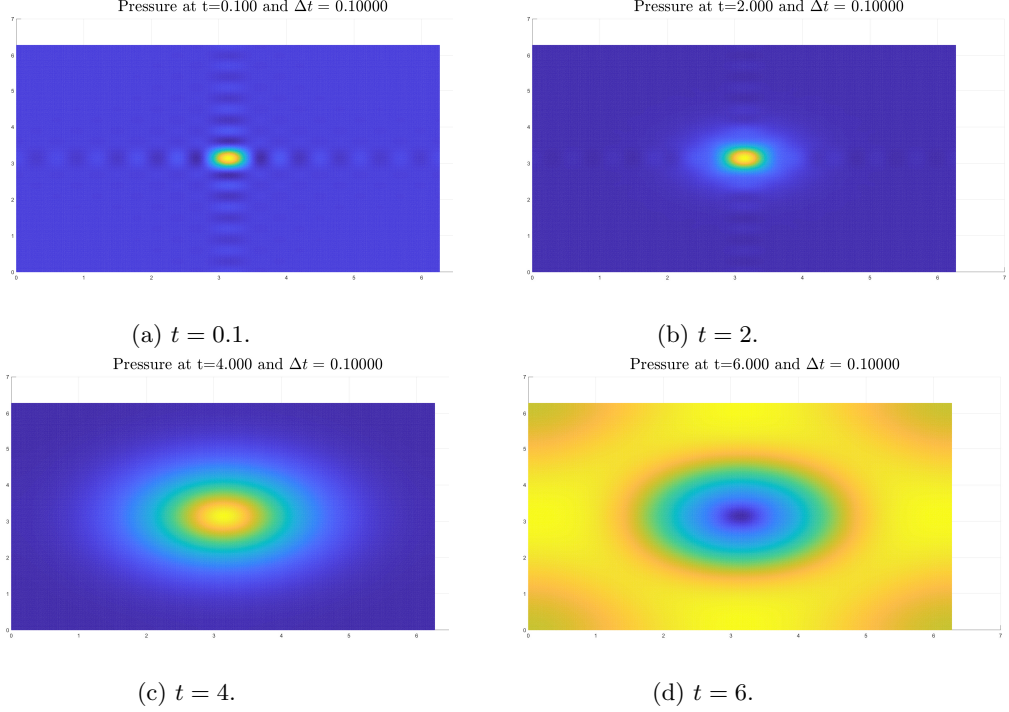

(a) $t = 0.1$.

(b) $t = 2$.

(c) $t = 4$.

(d) $t = 6$.

Figure 7: Wave propagation from Gaussian impact (19), computed by spatially enriched FEM centred at (π, π).

In Figure 7 we see that the short time plot propagates slowly from the epicentre but with a clear primary wave from the initial point. We then see the constant insult over time causes the rapid build up in energy over the whole domain (where $\Omega = [0, 2\pi]^2$), leaving the source term as a small less significant cause of pressure. Figure 8 quantifies the error of the numerical solution to problem (19). The error in the L^2-norm, evaluated at time t=1, decays with a rate of approximately 1 as the number of enrichment functions is increased. An error of less than 0.1% is achieved with fewer than 10 enrichments.
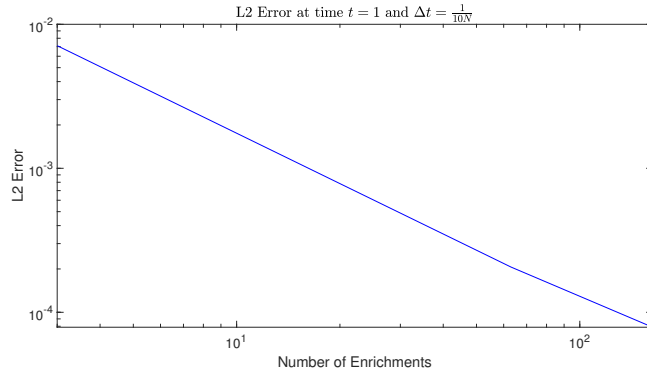

Figure 8: Convergence plot for the pressure.

Now consider the time enriched solutions for 21 integer enrichments between -10 and 10. Here we are taking the same right hand side but instead of considering a constant force at the centre we take an immediate impulse - consider a rock dropped into water. The result of the is that the pressure at the source is far larger compared to the other areas of the domain. As time progresses we see that the wave propagates radially in a uniform manner until the wavefront hits the boundaries of the region. Once the wave 'hits' the boundary we see that the periodic boundary conditions

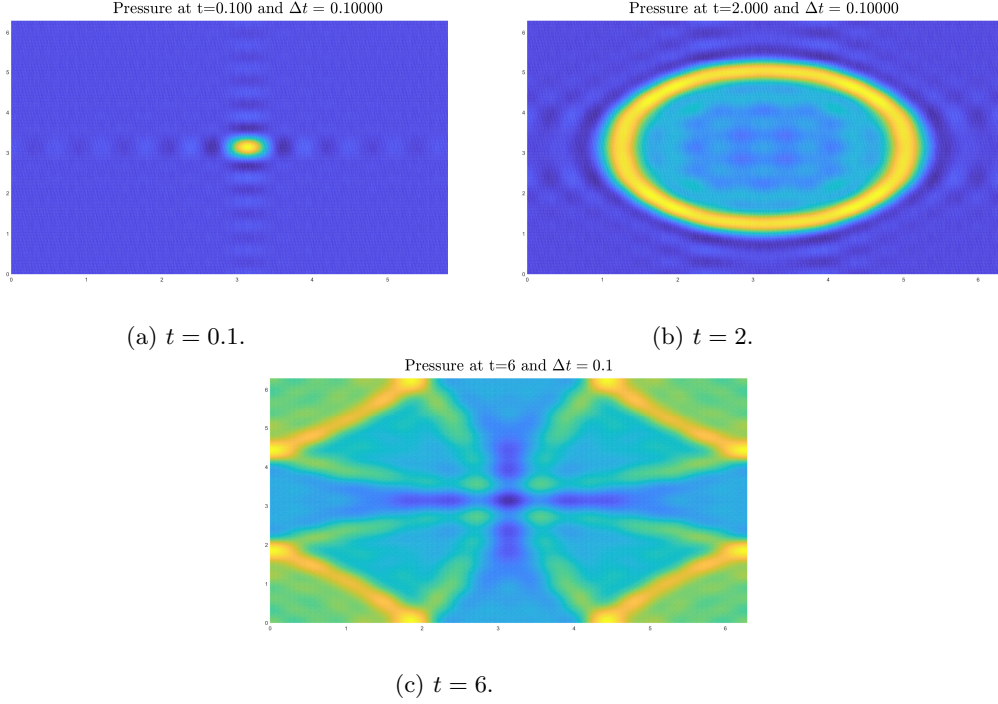(a) $t = 0.1$.   (b) $t = 2$.

(c) $t = 6$.

Figure 9: The time progression of the continuous Gaussian explosion over time for a space-time enriched FEM.

causes a symmetric reflection on each corner. This then leads to both constructive and destructive interference, as we see in Figure 9c. This phenomena could be associated with a wave impacting a hard surface and reflecting back into a material, in a simplified manner. This approach could be further expanded by placing hard blocks of material in the domain to see how to pressure interacts and reflects. Now that we have shown a brief example of a Gaussian impact, we should consider the error associated with the problem.
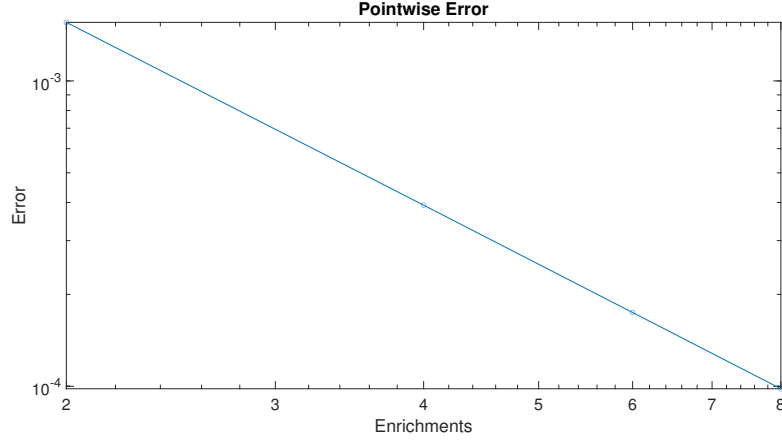
Figure 10: Pointwise error for enriched FEM. The time-step at each point is $\Delta t = \frac{1}{2N}$ for N the largest wavenumber.

Here we clearly see convergence in the pointwise regime of the enriched finite element scheme. We should also note that here we are taking substantially larger time steps, $\frac{1}{2N}$, compared to the time-independent case, $\frac{1}{10N}$, for N the largest wavenumber. Here we see that we can achieve a 0.01% error if we take our wavenumbers to range from -8 to 8, thus a total of 17 enrichments.

6   Acknowledgement

References

[1] Barucq, H., Calandra, H., Diaz, J. and Shishenina, E. [2017], 'Space-Time Trefftz - Discontinuous Galerkin Approximation for Elasto-Acoustics', (RR-9104).

[2] Bebernes, J. W. and Lacey, A. A. [2004], 'Shear band formation for a non-local model of thermo-viscoelastic flows'.

[3] Collino, F. and Tsogka, C. [2001], 'Application of the perfectly matched absorbing layer model to the linear elastodynamic problem in anisotropic heterogeneous media', *Geophysics* **66**, 294–307.

[4] Drolia, M., Mohamed, M. S., Laghrouche, O., Seaid, M. and Trevelyan, J. [2017], 'Enriched finite elements for initial-value problem of transverse electromagnetic waves in time domain', *Computers and Structures* **182**, 354–367.

[5] Ghantous, G. [n.d.], 'Beirut port blast death toll rises to 190'. Date Accessed: 17/09/20.
URL: https://www.reuters.com/article/us-lebanon-crisis-blast-casualties-idUSKBN25Q08H

[6] Gimperlein, H. and Stocek, J. [2019], 'Space–time adaptive finite elements for nonlocal parabolic variational inequalities', *Computer Methods in Applied Mechanics and Engineering* **352**, 137 – 171.
URL: http://www.sciencedirect.com/science/article/pii/S0045782519302221

[7] Hager, C., Hauret, P., Le Tallec, P. and Wohlmuth, B. I. [2012], 'Solving dynamic contact problems with local refinement in space and time', *Computer Methods in Applied Mechanics and Engineering* **201-204**, 25 – 41.
URL: http://www.sciencedirect.com/science/article/pii/S0045782511002957

[8] Iqbal, M., Gimperlein, H., Mohamed, M. S. and Laghrouche, O. [2017], 'An a posteriori error estimate for the generalized finite element method for transient heat diffusion problems', *International Journal for Numerical Methods in Engineering* **110**(12), 1103–1118.
URL: https://onlinelibrary.wiley.com/doi/abs/10.1002/nme.5440

[9] Iqbal, M., Stark, D., Gimperlein, H., Mohamed, M. and Laghrouche, O. [2020], 'Local adaptive q-enrichments and generalized finite elements for transient heat diffusion problems', *Computer Methods in Applied Mechanics and Engineering* **372**, 113359.
URL: http://www.sciencedirect.com/science/article/pii/S0045782520305442

[10] Laghrouche, O., Bettess, P., Perrey-Debain, E. and Trevelyan, J. [2005], 'Wave interpolation finite elements for Helmholtz problems with jumps in the wave speed', *Computer Methods in Applied Mechanics and Engineering* **194**(2), 367 – 381.
URL: http://www.sciencedirect.com/science/article/pii/S0045782504003378

[11] Larson, M. and Bengzon, F. [2013], *The Finite Element Method: Theory, Implementation, and Applications*, Texts in Computational Science and Engineering, Springer Berlin Heidelberg.
URL: https://books.google.co.uk/books?id=Vek_AAAAQBAJ

[12] Ma, D., Chen, P., Dai, K. and Zhou, Q. [2014], 'Specimen size effect of explosive sensitivity under low velocity impact', *Journal of Physics: Conference Series* **500**(5), 052026.
URL: https://doi.org/10.1088%2F1742-6596%2F500%2F5%2F052026

[13] Moiola, A. and Perugia, I. [2018], 'A space–time Trefftz discontinuous Galerkin method for the acoustic wave equation in first-order formulation', *Numerische Mathematik* **138**(2), 389–435.

[14] Perrey-Debain, E., Trevelyan, J. and Bettess, P. [2005], 'On wave boundary elements for radiation and scattering problems with piecewise constant impedance', *IEEE Transactions on Antennas and Propagation* **53**(2), 876–879.

[15] Peter Hicks, C. H. [n.d.], 'Modelling of the effects of friction andcompression on explosive'.

[16] Petersen, S., Farhat, C. and Tezaur, R. [2009], 'A space–time discontinuous galerkin method for the solution of the wave equation in the time domain', *International Journal for Numerical Methods in Engineering* **78**(3), 275–295.
URL: https://onlinelibrary.wiley.com/doi/abs/10.1002/nme.2485

[17] Prothero, M. [2020], 'Lebanon is running out of food after the beirut explosion wrecked its main port — leaving a bottleneck for supplies that may see the country go hungry'. Date Accessed: 17/09/20.
URL: https://www.businessinsider.com/lebanon-food-shortages-beirut\ -blast-wrecks-port-bottleneck-crisis-2020-8?r=US&IR=T

[18] Thomée, V. [2006], *Galerkin finite element methods for parabolic problems*, Vol. 25 of *Springer Series in Computational Mathematics*, Springer Berlin Heidelberg.